Cao, C., Burgess, S., & Conn, A. T. (2018). Flapping at resonance: Realization of an electroactive elastic thorax. In *2018 IEEE International Conference on Soft Robotics (RoboSoft 2018): Proceedings of a meeting held 24-28 April 2018, Livorno, Italy* (pp. 327-332). Institute of Electrical and Electronics Engineers (IEEE). https://doi.org/10.1109/ROBOSOFT.2018.8404940

Flapping at resonance: realization of an electroactive elastic thorax

Chongjing Cao[1], Stuart Burgess[2], and Andrew T. Conn[1,2 a)]

***Abstract*—Insect-inspired flapping wing micro air vehicles (MAV) have attracted considerable interest due to their potential for agile flight in complex environments. Resonant excitation of the wing flapping mechanism in insects is highly advantageous as it amplifies the flapping amplitude and reduces the inertial power demand. Dielectric elastomer actuators (DEA) produce large actuation strain and their inherent elasticity is ideal for resonant operation. In this work we present a double cone DEA design and characterize its resonant frequency and phase shift to analyze its mechanical power output as a DEA-mass oscillator. Then an artificial thorax driven by this elastic actuator is demonstrated, this thorax design is able to provide a peak flapping amplitude of 63° at a frequency of 18 Hz.**

I. Introduction

Insect inspired flapping wing micro air vehicles (MAVs) have drawn great interest in recent years for their potential for highly agile flying robots. Many MAV designs have achieved either tethered or untethered flight and some of the well-known designs include Microrobotic Fly [1], DelFly [2] and Robotic hummingbird [3]. However, the practical realization of these flapping wing MAVs has been limited by the extremely high power demands required for autonomous flight at micro scales. Insects take advantage of their elastic thorax and muscle system as a damped oscillator and flap their wings at its resonant frequency [4]. Most species of flying insect use indirect dorsoventral (dvm) and dorsolateral (dlm) muscles to elevate and depress their wings respectively [5] (Figure 1 (a) and (b)). The muscles are described as indirect as they manipulate the top plate of the thorax, known as the notum, which drives the wings through the pleural wing process. This highly elastic natural oscillator enables resonant excitation to take advantage of the amplified the flapping stroke and greatly reduced inertial power demands [4]. Due to the constraints of incorporating elasticity into conventional robotic technologies, only few attempts have been made to integrate resonant excitation into flapping wing MAVs. By adding a spring to a motor driven flapping mechanism, [6] showed a 30% average power reduction by driving at resonant frequency. In contrast, the most notable example of an integrated resonant oscillator is the Microrobotic Fly, which is a 60 mg robotic insect powdered by piezoelectric actuator at the resonant frequency of this system of 110 Hz [1].

Emerging soft robotic actuation technologies such as dielectric elastomer actuators (DEAs) offer an alternative paradigm for flapping wing MAV designs. Firstly, DEAs achieve large actuation strains that are similar to muscles. Secondly, the inherent elasticity of the material makes DEAs capable of storing and releasing inertial energy, like the highly efficient elastomeric protein (resilin) found in the thorax of insects does [7]. These characteristics make DEA an ideal candidate to achieve an artificial elastic thorax that acts as a resonant oscillator seen in insects. Finally, DEAs have good scaling capability. Apart from miniaturization and increasing the active area to generate larger stroke and higher power output, multiple layers of DEA membranes can be added in parallel to exert lager force and power with a minimal effect on the size of the actuator. Very few DEA driven flapping wing mechanisms have been developed to date. Lau and co-workers [8] [9] tried rolled and stacked DEAs to drive the wings and their two designs have been demonstrated only to be able to flap 10° and 2° at 1 Hz. By using a minimum energy structure, [10] have demonstrated a dragonfly-like flapping robot and the flapping stroke is estimated to be about 15°. The stroke and frequency of the aforementioned DEA driven flapping mechanisms are far from being high enough to enable flight, as insects have a typical stroke of 120° and frequencies of 20-40 Hz for the largest insects to over 200 Hz for smaller species [11]. Thus in this work, we present an electroactive elastic thorax design which seeks to achieve a larger stroke amplitude and wingbeat frequency. Figure 1 (c) and (d) show the design concept of the elastic thorax driven by a linear DEA.

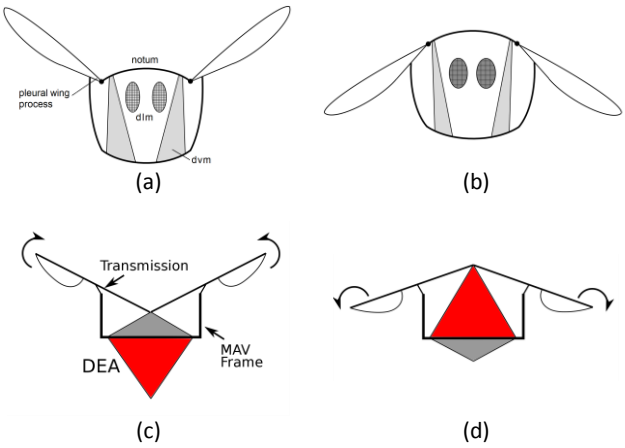

Figure 1. Transverse view of the thorax showing the indirect dorsoventral (dvm) and dorsolateral (dlm) muscles elevating (a) and depressing (b) the wings respectively, via the notum and pleural wing process (redrawn from [5]). (c) and (d), proposed elastic thorax where DEA is attached to the frame and drives the

1. Bristol Robotics Laboratory, Bristol. BS16 1QY. United Kingdom.
2. Department of Mechanical Engineering. University of Bristol. Queens Building, University Walk, BS8 1TR. United Kingdom.

a). Corresponding author: a.conn@bristol.ac.uk

This paper is organized as follows. In section II, the double cone linear actuator is introduced. In section III, we compare the performance of two types of elastomer for DEA with respect to high frequency domain at which insect inspired MAV operate. By using a DEA-mass system as an oscillator, in sections IV and V we characterize the natural frequency of this oscillator and the mechanical power output at resonance respectively. Then in section IV the flapping motion of this elastic thorax at its resonant frequency is demonstrated. Finally, conclusions and future work are discussed.

II. Double Cone Linear DEA Design

In this work, we employ a double cone DEA configuration [12] [13] and the general incorporates two dielectric elastomer membrane that are separately bonded to two circular frames with a protrusion from a strut pushing the centre of the membranes to form a double cone shape, as shown in Figure 2. The advantage of a double cone design is its natural agonist-antagonist configuration as the two single conical DEA membranes can be actuated separately to produce bidirectional actuation. It also has a good compactness, high mass-specific energy density and can be fabricated consistently. The actuation of a double cone DEA depends on the balance of forces exerted by the two deformed DEA membranes on the strut. When no actuation voltage is applied, each membrane exerts an equal reaction force on the strut, and the strut balances in the middle. However, when a voltage difference is applied across the electrodes of one DEA membrane, the generated Maxwell stress and resultant planar membrane expansion drives the strut towards the actuated membrane side. As the Maxwell stress is directly related to the voltage applied to the DEA, voltages in the range of 1 to 10 kV are usually used. For a challenge for DEA driven MAV application would be to develop miniature high voltage amplifiers. On the other hand, electro-mechanical efficiency of a real DEA, which describes the ratio between the mechanical work output and the electrical energy input of the actuator, has been shown to be significantly lower than the theoretical estimation [14]. This is partially due to the fact that most of the existing high voltage amplifier cannot recover the electric energy stored in DEA as in the theoretical estimation. Hence an integrated miniature amplifier that can recover electric energy is demanding.

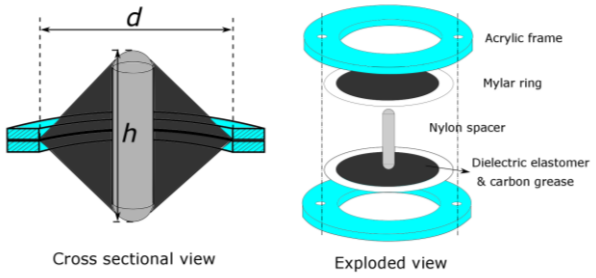

Figure 2. Schematic design of the double cone actuator with inner ring diameter, *d*, and spacer height, *h*, labeled.

Silicone elastomers and polyacrylate tape VHB (3M) are the two predominant DEA materials. VHB is known for its large energy density and actuation strain [15], its inherent adhesiveness and wide commercial availability which make it widely adopted for DEA prototyping. On the other hand, silicone elastomers typically have a lower viscosity, which makes them suitable for fast actuation applications such as MAVs where the frequency is usually over 10 Hz. In this work, we adopt VHB 4905 and an off the shelf silicone membrane (PARKER EAP 40 µm) and compare their respective performance.

The fabrication process of the double cone DEAs is described as follows. For VHB based actuators, each 0.5 mm thick VHB 4905 membrane was given a biaxial pre-stretch of 4×4 and bonded directly to a 2 mm thick acrylic ring frame with an inner diameter *d*. The silicone membrane actuators followed a similar first step, except that each 40 µm membrane was bonded to 0.1 mm thickness Mylar rings using silicone adhesive (Smooth-On Sil-Poxy) without any pre-stretch and then attached to the acrylic ring frame. The choice of having no pre-stretch is mainly because protrusion from the strut can introduce significant stretch on the membrane, which is believed sufficient for silicone elastomers. Carbon conductive grease (M.G. Chemicals Ltd) was hand brushed onto each side of the membrane as the compliant electrodes and copper tape was used as a connection between compliant electrodes and high voltage cables. Finally, the two circular frames were fixed together by nylon fasteners. One nylon spacer with a dome cap on each end and a height *h* was used as the support strut to maintain the tension on the DEA membranes. Figure 2 shows the preassembled components of the DEA in an exploded view.

III. Actuator Material Characterization

The dynamic performance of the double cone DEAs can be characterized by the free stroke as a function of the excitation frequency and they were tested by following the protocol suggested in [16] and is described as follows. First, two double cone DEA specimens were prepared, one using silicone membrane and the other one using VHB 4905. The inner diameter of the actuator *d* is 40 mm and the strut height *h* is 30 mm. The rigid acrylic frames of the actuator were clamped to a testing rig, which left the nylon spacer to move freely. For each specimen, the two single conical membranes were driven by separate sinusoidal voltages with an amplitude of 1920 V for silicone membranes and 2500 V for VHB pairs. The two sinusoidal voltages are 180° out of phase such that the actuator can achieve antagonistic actuation. Actuation voltage signals with frequencies from 1 to 100 Hz were generated using MATLAB, via a DAQ (National Instruments BNC-2111) and amplified using a high voltage amplifier (Ultravolt 5HVA23-BP1). The displacement of the end-effector (nylon spacer in this case) was measured by a laser displacement sensor (LK-G152 and LKGD500, Keyence). 50 cycles were repeated at each frequency to allow the actuator to reach a steady state.

The amplitudes of the stroke and the phase differences between the input voltage and the stroke were analysed and the results are shown in Figure 3 (a) and (b). Both silicone and VHB specimens generate a stroke of 2 mm at 1 Hz. For silicone DEA, two peaks occur at 20 and 52 Hz respectively, where the second is believed to be the mechanical resonance

frequency. The amplitude of the VHB specimen reduces continuously with the increasing actuation frequency, which is due to the significantly viscous behaviour of the elastomer. From the phase response plot, a 90° phase shift is found at 52 Hz for both silicone and VHB specimens, which proves that 52 Hz is the mechanical resonant frequency for this silicone DEA. It is also suggested by [16] that, for high viscous damping materials which have no amplitude peak, the resonant frequency can be determined by the value that causes a phase shift of 90°. The superior performance of the silicone DEA at high frequencies over VHB suggests that the low viscous damping silicone elastomer can be used in high frequency applications and achieve resonant excitation. In later sections, the mechanical power of the silicone DEA will be investigated to analyse its feasibility in resonant excitation flapping wing MAV designs. While the optimization of mechanical impedance through phase shift analysis is focused on flapping wing MAVs here, this general approach has wider application to any soft robotic devices driven by periodic excitation.

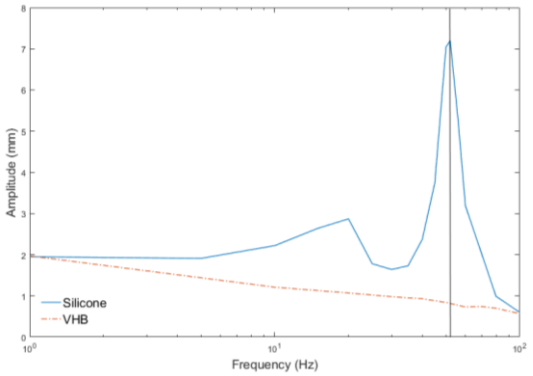

Figure 3. Dynamic characterization of the silicone and VHB DEA. (a) Amplitudes of the silicone and VHB specimen as a function of actuation frequency; (b) phase difference between the driving signal and stroke output of the silicone and VHB specimen as a function of actuation frequency.

IV. Double Cone DEA Resonance Characterization

In a classical mechanical undamped oscillator, its natural frequency f_0 can be expressed as $f_0 = \frac{\sqrt{K/M}}{2\pi}$, where K is the stiffness of the spring and M is the mass. Double cone DEA has been shown to have an approximately constant stiffness despite the non-linear material properties [17], so in this work we assume that the DEA is a linear spring. By considering the mass of the spacer and any payload as M in the undamped oscillator (assuming the mass of the DEA membranes is negligible), we are able to predict the resonant frequency of the DEA-mass oscillator. It should be noted that here we assume the damping ratio of the silicone DEA is small enough to be neglected in the natural frequency characterization, and the good agreement between the prediction and experimental results suggests that this assumption holds.

To verify the feasibility of using the standard mechanical oscillator theory to predict the resonant frequency of a silicone double cone DEA-mass system, five specimens were prepared with different stiffness and mass values. The stiffness of these specimens were adjusted by using different spacer height to frame diameter h/b ratio (refer to Fig. 2) and adding an additional layer. The stiffness of each DEA was estimated by pushing the DEA against a load cell (KYOWA, LMA-A-10N). The reaction force against displacement of the DEA was linear fitted with a coefficient of determination R^2 = 0.9998, which suggests that the stiffness of the DEA can be approximated as a constant value. The detailed values of the stiffness and mass, the predicted and measured resonant frequencies of these five specimens are listed in Table I. The prediction agrees very well with the experimental results, with an average relative error of 1.98 %, which confirms that the damping ratio of this silicone DEA is negligible. It can also be noticed that the DEAs with heavier payload and lower stiffness exert larger strokes at their resonant frequencies as a result of the kinetic and potential strain energy being stored and released.

TABLE I. Experimental results for the DEA-mass oscillator resonant frequency characterization.

	DEA 1	**DEA 2**	**DEA 3**	**DEA 4**	**DEA 5**
***K* (N/m)**	63.5	63.5	63.5	41.4	127
***M* (g)**	0.603	1.26	2.538	1.26	1.26
***d* (mm)**	7.2	8.8	9.35	10.85	8.12
f_0 predicted (Hz)	51.8	35.7	25.2	28.8	50.5
f_0 measured (Hz)	52	37	26	28	51
Relative error of f_0	0.39 %	3.64 %	1.98 %	2.9 %	0.98 %

V. Maximizing Actuator Power Output

A. Multiple layer actuator

With the largest stroke at its resonant frequency, the silicone double cone DEA has the potential to produce a higher power output than VHB 4905. In this section, we investigate the power of the DEA as a function of actuation frequency. In addition to exploiting resonance, multiple layers of DEA membranes can be stacked to produce a greater power. So by fixing the resonant frequency, we also compare the power output as a function of the number of layers. A mass is attached to the strut as a payload, so the instant

mechanical power output is considered as $P_{mech} = M\frac{d^2x}{dt^2}\frac{dx}{dt}$, where M is the mass, x is the displacement of the mass and t is time. The average mechanical power output is simply $P_{mech\_avg} = \frac{1}{T}\int_0^T P_{mech}\,dt$, where T is the period of one actuation cycle.

B. Experiment

The size of the double cone DEA is reduced here to make it more suitable for real flapping wing MAV applications. The frame diameter d is 26 mm and the spacer height h is 13 mm.

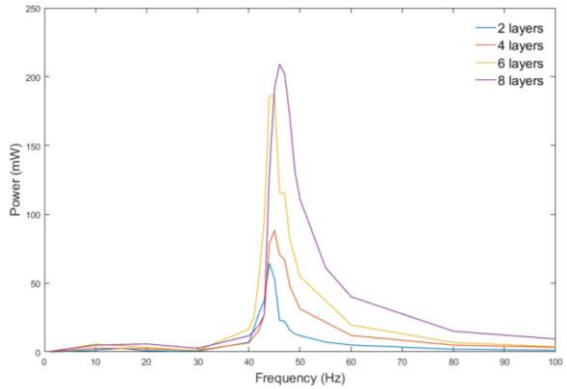

Figure 4. Average mechanical power as a function of frequency for 2, 4, 6 and 8 layers of double cone silicone DEAs.

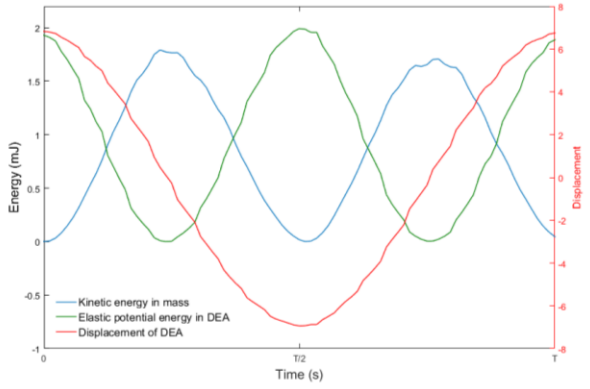

Figure 5. Kinetic energy and elastic potential energy in the DEA-mass system at its resonance.

2, 4, 6 and 8 layers of silicone membranes were tested and the payload for each specimen is 1, 2, 3 and 4 grams respectively, which results in a similar resonant frequency of 45.8 Hz. Each layer of the membrane including Mylar ring frame, carbon grease electrode and copper tape connection weighs 0.12 g.

Figure 4 shows the measured average mechanical power from the actuator as a function of frequency. It can be noticed that very low power was exerted by the DEA in the low frequency region (< 35 Hz), while the average power output rises rapidly and peaks at the resonant frequency. The high average mechanical power output of the DEA at its resonance can be explained by the elastic energy stored in the DEA being close to 90° out of phase with the kinetic energy of the mass, which indicates that in the beginning of each half stroke, the elastic energy of the DEA membranes converts into the kinetic energy of the mass, which helps to accelerate the mass faster, hence a larger mechanical power (Figure 5). At the end of each half stroke, the kinetic energy of the mass is converted into the elastic potential energy in the membranes, which is then released in the next half cycle. This increases the efficiency of the DEA, see [17] for a detailed elastic energy recovery study on double cone DEAs. By comparing the maximum average power output of the DEAs of 4, 6 and 8 layers of silicone membranes with the 2-layer specimen within the actuation frequency from 1 to 100 Hz from Table II, the maximum average mechanical power scaled up as expected. Due to the increase in capacitance and the connection issue between DEA electrodes and high voltage channels, the 8-layer specimen did not generate as high as four times average mechanical power as the 2-layer one. The mass specific power for these DEAs are about 100 mW/g at its maximum. By comparison, insect flight muscle is estimated to have a mass specific power of 80 to 83 mW/g [18] [19], and a typical piezoelectric actuator has a mass specific power of 400 mW/g [20]. Despite the high mass specific power, piezoelectric actuators have very low strokes (< 1%) and only achieves high power at high frequencies (generally > 100 Hz) [21]. On the other hand, the double cone DEA adopted in this work has a mass specific power close to insect muscle, and an actuation frequency close to the flapping frequencies of large to medium insects, which makes it a suitable candidate for bio-inspired flapping wing MAV applications.

TABLE II. Maximum average mechanical power within 1-100 Hz actuation frequencies and mass-specific power of 2, 4, 6 and 8 layers of double cone silicone DEA.

Number of layers n	**2**	**4**	**6**	**8**
P_{max} **(mW)**	64.49	88.38	186.6	209.1
P_{max} / P_{max}**(n = 2)**	100 %	137 %	289 %	324 %
Mass-specific power **(mW/g)**	134.35	92.06	129.58	108.91

VI. Elastic Thorax Design

A. Design overview

To demonstrate the feasibility of using the double cone DEA to flap the wings at resonance, an artificial thorax is designed in this work where the elasticity is embedded in the DEA itself, hence no additional elastic element is required. The elastic thorax consists of the DEA actuator and a flapping mechanism, which includes a slider crank mechanism to convert the linear motion of the DEA end-effector into a reciprocal flapping motion and a double rocker mechanism connected in series to amplify this motion. Two mechanical stops are included to the slider to avoid singularities in the mechanism. A schematic diagram of this design is illustrated in Figure 6 and the design parameters are listed in Table III. It should be noted that the aim of this design is to prove the

concept in benchtop tests and hence the size and weight of this mechanism are not optimized for free flight.

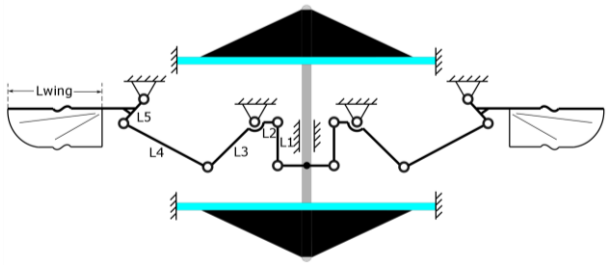

Figure 6. Schematic design of the elastic thorax (not to scale).

TABLE III. Design parameters and values for the elastic thorax.

Parameter	L_1	L_2	L_3	L_4	L_5	L_{wing}
Value (mm)	8	4	8.5	18	5	40

B. Elastic thorax flapping tests

An 8-layer double cone DEA with silicone elastomer membranes d = 26 mm and h = 13 mm was used. Two square waves with an amplitude of 1920 V and 180° phase shift were used to drive the antagonistic DEA membranes. An actuation frequency of up to 60 Hz was tested.

In the first test, no wing was attached, which left the DEA driving the mechanism only. The rotational stroke of this mechanism increases with the increasing actuation frequency and a clear peak is seen at 34 Hz in Figure 7. As the frequency increases further above 34 Hz the stroke begins to reduce, which is due to the inertia of the linkages and frictional loss.

In the second test, only the wing frames were connected to the flapping mechanism, which adds the inertia of the wings but not aerodynamic forces to this system. The inertia of the wings does not affect the flapping stroke much at frequencies below resonance, however, it lowers the resonant frequency from 34 Hz to 22 Hz, and gives a smaller flapping stroke of 83° (Figure 7). Above the resonant frequency, the flapping stroke reduces sharply with the frequency.

In the final test, wing membranes are included, which introduces the aerodynamic drag. The aerodynamic force reduces the peak flapping stroke, which is 63° at 18 Hz. In Figure 8, the flapping motion of the complete elastic thorax is demonstrated. Based on the following empirical equation which describes the mass that can be supported during hovering from [4], the current prototype can generate a lift of about 133 mg.

$$m = 0.387 \frac{\phi^2 n^2 R^4 C_L}{AR},$$

where m is mass (kg), ϕ is flapping stroke (rad), n is frequency (Hz), R is the wing length (m), C_L is the lift coefficient (C_L = 2 to 3 for insect hovering) and AR is the aspect ratio.

To generate sufficient lift for a 10 g MAV to achieve hovering, assuming the stroke amplitude is ϕ = 120° and AR = 7 (commonly seen in flying insects [4]), the MAV has to flap at 100 Hz for a wing length of 40 mm or at 20 Hz for a wing length of 80 mm. For multi-layer DEAs with large capacitance, it is favorable to operate them at relatively low frequencies which will allow sufficient charging and discharging periods. Hence a DEA driven MAV with low flapping frequency and a pair of long wings are preferred. Several key areas of further development will be (i). Improved electrode conductivity using alternative materials such as carbon nanotubes (such as in [22]). It is anticipated that this will improve the electrical response of the actuator thus increasing the power output. (ii). Optimizing the coupling between the DEA and flapping mechanism so that long wings are used and the resonant frequency is selected at a relatively low value (say 15-25 Hz). (iii). Optimizing the flapping mechanism in terms of transmission speed ratios by adjusting the link ratios.

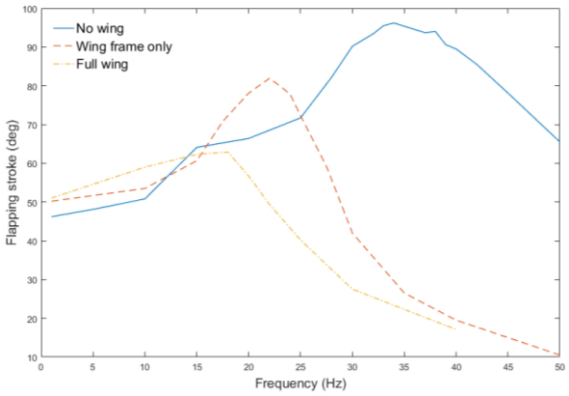

Figure 7. Flapping strokes of the elastic thorax as a function of frequency with no wing attached, wing frames only and full wings attached.

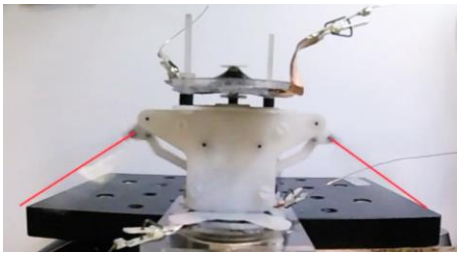

(i) Wings at the bottom end

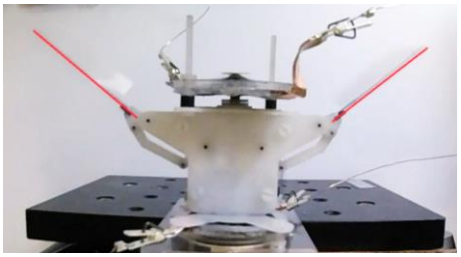

(ii) Wings at the top end

Figure 8. Flapping motion of this elastic thorax at 18 Hz. (video: https://youtu.be/UU6Jgo5GVnA)

VII. Conclusion

In this work, we present an elastic thorax design inspired by insects. First, we develop a DEA-mass oscillator to show that a highly elastic double cone DEA can be driven at resonance to significantly boost the stroke amplitude and mechanical power output. Its natural frequency can be estimated by the classic oscillator model to enable DEA design optimization. The mechanical power output of this actuator was shown to have a peak at the predicted resonant frequency of the system and this value scaled up with the number of layers of DEA membranes in the actuator. By driving the DEA-mass system at its resonant frequency, we demonstrate a 209.1 mW average mechanical power output and an equivalent of 108.9 W/kg mass-specific mechanical power density from an 8-layer DEA. Subsequently, we show that the insect-inspired wings can have a peak flapping stroke of 63° at 18 Hz. While this flapping performance requires further optimization towards generating enough lift for flight, this prototype far outperforms previous DEA-based flapping mechanisms in terms of stroke amplitude and wingbeat frequency e.g. a stroke amplitude of 15° in [10] and 10° at a frequency of 5 Hz in [8]. In the future work, we will continue working on optimizing the actuator and the flapping mechanism. A dynamic electro-mechanical model for the double cone DEA will be developed to help us quantify its natural frequency and power output. Future versions of the prototype can be developed by, for example, the smart composite microstructures fabrication technique from [1] which will have ultra light weight yet strong flapping mechanism to reduce the overall weight of the MAV and hence reduce the power requirement from the DEA and even potentially allow onboard control and sensing systems.

Acknowledgment

This work was supported by the EPSRC centre for doctoral training in Future Autonomous and Robotic Systems (FARSCOPE) at the Bristol Robotics Laboratory where C.C. is a PhD student. A.C. was supported by EPSRC grant EP/P025846/1.

VIII. References

[1] R. J. Wood, "The first take off of a biologically inspired at-scale robotic insect.," *IEEE transcations on robotics*, pp. 24(2), 341-347, 2008.

[2] G. De Croon, K. De Clercq, R. Ruijsink, B. Remes and C. de Wagter, "Design, aerodynamics, and vision-based control of the DelFly," *International Journal of Micro Air Vehicles*, vol. 1, no. 2, pp. 71-97, 2009.

[3] M. Keennon, K. Klingebiel, H. Won and A. Andriukov, "Development of the nano hummingbird: A tailless flapping wing micro air vehicle.," in *n AIAA aerospace sciences meeting*, Reston, 2012.

[4] C. P. Ellington, "The novel aerodynamics of insect flight: applications to micro-air vehicles," *Journal of Experimental Biology*, vol. 23, no. 202, pp. 3439-3448, 1999.

[5] J. Pringle, Insect flight, Cambridge: Cambridge University Press, 1957.

[6] S. S. Baek, K. Y. Ma and R. S. Fearing, "Efficient resonant drive of flapping-wing robots," in *Intelligent Robots and Systems, IROS 2009. IEEE/RSJ International Conference on*, St. Louis, MO, USA, 2009.

[7] R. Dudley, The biomechanics of insect flight: form, function, evolution, Princeton University Press, 2002.

[8] G. K. Lau, H. T. Lim, J. Y. Teo and Y. W. Chin, "Lightweight mechanical amplifiers for rolled dielectric elastomer actuators and their integration with bio-inspired wing flappers," *Smart Materials and Structures*, vol. 2, no. 23, p. 025021, 2014.

[9] G. K. Lau, Y. W. Chin and T. G. La, "Development of elastomeric flight muscles for flapping wing micro air vehicles," in *Electroactive Polymer Actuators and Devices (EAPAD) 2017*, Portland, 2017.

[10] E. Henke, K. Wilson and I. Anderson, "Entirely soft dielectric elastomer robots," in *Electroactive Polymer Actuators and Devices (EAPAD) 2017*, 2017.

[11] A. K. Brodsky, The Evolution of Insect Flight, Oxford: Oxford University Press, 1994.

[12] H. R. Choi, K. M. Jung, J. W. Kwak, S. W. Lee, H. M. Kim, J. W. Jeon and J. D. Nam, "Digital polymer motor for robotic applications," in *Robotics and Automation, 2003. ICRA'03. IEEE International conference on*, 2003.

[13] A. T. Conn and J. Rossiter, "Towards holonomic electro-elastomer actuators with six degrees of freedom," *Smart Materials and Structures*, vol. 3, no. 21, p. 035012, 2012.

[14] J. Bigué and J. Plante, "Experimental Study of Dielectric Elastomer actuator energy conversion efficiency.," *IEEE/ASME Transactions on Mechatronics*, vol. 1, no. 18, pp. 169-177, 2013.

[15] F. Carpi, R. Kornbluh, P. Sommer-Larsen and G. and Alici, "Electroactive polymer actuators as artificial muscles: are they ready for bioinspired applications?," *Bioinspiration & biomimetics*, vol. 4, no. 6, p. 045006, 2011.

[16] F. Carpi, I. Anderson, S. Bauer, G. Frediani, G. Gallone, M. Gei, C. Graaf, C. Jean-Mistral, W. Kaal, G. Kofod and M. Kollosche, "Standards for dielectric elastomer transducers," *Smart Materials and Structures*, vol. 10, no. 24, p. 105025, 2015.

[17] C. Cao and A. T. Conn, "Elastic actuation for legged locomotion," in *Electroactive Polymer Actuators and Devices (EAPAD) 2017*, Portland, 2017.

[18] F. Lehmann and M. Dickinson, "The changes in power requirements and muscle efficiency during elevated force production in the fruit fly Drosophila Melanogaster," *Journal of Experimental Biology*, vol. 7, no. 200, pp. 1133-1143, 1997.

[19] M. Tu and T. Daniel, "Submaximal power output from the dorsolongitudinal flight muscles of the hawkmoth Manduca sexta," *Journal of Experimental Biology*, vol. 26, no. 207, pp. 4651-4662, 2004.

[20] E. Steltz and R. Fearing, "Dynamometer power output measurements of piezoelectric actuators," in *In Intelligent Robots and Systems, 2007. IROS 2007. IEEE/RSJ International Conference on. IEEE*, 2007.

[21] J. Huber, N. Fleck and M. Ashby, "The selection of mechanical actuators based on performance indices," in *Royal Society of London A: Mathematical, Physical and Engineering Sciences*, 1997.

[22] W. Yuan, H. L. B. Z. B. Yu, T. Lam, J. Biggs, S. M. Ha, D. J. Xi, B. Chen, M. K. Senesky, G. Grüner and Q. Pei, "Fault‐Tolerant Dielectric Elastomer Actuators using Single‐Walled Carbon Nanotube Electrodes," *Advanced Materials*, vol. 3, no. 20, pp. 612-625, 2008.